



Time-triggered and event-triggered control of switched affine systems via a hybrid dynamical approach

Carolina Albea-Sanchez, Alexandre Seuret

► To cite this version:

Carolina Albea-Sanchez, Alexandre Seuret. Time-triggered and event-triggered control of switched affine systems via a hybrid dynamical approach. 2019. hal-02336728v1

HAL Id: hal-02336728

<https://laas.hal.science/hal-02336728v1>

Preprint submitted on 29 Oct 2019 (v1), last revised 16 Mar 2021 (v2)

HAL is a multi-disciplinary open access archive for the deposit and dissemination of scientific research documents, whether they are published or not. The documents may come from teaching and research institutions in France or abroad, or from public or private research centers.

L'archive ouverte pluridisciplinaire **HAL**, est destinée au dépôt et à la diffusion de documents scientifiques de niveau recherche, publiés ou non, émanant des établissements d'enseignement et de recherche français ou étrangers, des laboratoires publics ou privés.

Time-triggered and event-triggered control of switched affine systems via a hybrid dynamical approach

Carolina Albea Sanchez^{a,*}, Alexandre Seuret^a

^aLAAS-CNRS, Université de Toulouse, CNRS, UPS, 7 avenue du Colonel Roche, 31031 Toulouse, France

Abstract

This paper focuses on the design of both periodic time- and event-triggered control laws of switched affine systems using a hybrid dynamical system approach. The novelties of this paper rely on the hybrid dynamical representation of this class of systems and on a free-matrix min-projection control, which relaxes the structure of the usual Lyapunov matrix-based min-projection control. This contribution also presents an extension of the usual periodic time-triggered case to the event-triggered one, where the control updates are permitted only when a particular event is detected. Together with the definition of an appropriate optimization problem, a stabilization result is formulated to ensure the uniform global asymptotic stability of an attractor for both types of controllers, which is a neighborhood of the desired equilibrium. Finally, the proposed method is evaluated through a numerical example.

Keywords: Switched-affine systems, periodic time-triggered control, aperiodic event-triggered control, hybrid dynamical systems, Lyapunov stability, dwell time.

1. Introduction

Switched affine systems [1] are encountered in many applications including DC-DC power conversion [2, 3], biochemical networks [4], aerospace [5] and urban traffic [6]. This class of systems is characterized by the fact that the
5 origin is not necessarily a common equilibrium of all operating modes. This usually prevents from the asymptotic stabilization to this common equilibrium. Indeed, the set of operating points are given by a dynamic averaging, obtaining solutions in the generalized sense of Krasovskii. Many papers can be found in the literature on controlling continuous-time switched affine systems. This is
10 usually achieved thanks to the Lyapunov matrix-based min-projection control strategy [7, 8] and several contributions succeeded in applying this strategy to the control of DC-DC power converters [9, 10] and even comprising experimental

*Corresponding author

results [11, 12]. Moreover, this Lyapunov-based controller was also applied to a more general class of nonlinear switched systems [13].

15 It is worth noting that this control strategy suffer from a major drawback in continuous time. Indeed, it may lead to arbitrarily fast switching control signals, generating eventually a Zeno solution. Therefore several contributions aimed at ensuring a minimum dwell-time solution with an admissible chattering around the operating point. To cite only the ones focusing on power converters, the
 20 authors of [14] imposed a minimum dwell time, thanks to a time regularization. The solution presented in [3] focused on the specific classical boost converter and [15] does not provide a stability proof. Likewise, the authors of [16] have provided a solution to the control of switched affine systems that avoids Zeno behavior using both time- and space-regularization and a hybrid dynamical
 25 system formulation. Moreover, propositions for an extended formulation of these systems in nonlinear systems are given in [17, 18].

In many occasions, the control law has to be implemented periodically in a time-triggered method, as it is generally encountered in electronics [19, 20]. Moreover, this periodic implementation constraint also represents a challenge
 30 in other fields, as in aerospace [21] or in robotic [22, 23]. In order to deal with this issue, a solution consisting in the discretization of a continuous-time model gathering the fact that the control law is periodically updated was provided in [24, 25, 26]. However, these results disregard the trajectories between two sampling, preventing to provide a complete analysis of the continuous trajectories
 35 of the system. Compared to the continuous-time approach, the discrete one has the advantage to disregard the problem of Zeno behavior since it inherently includes a dwell time constraint.

Switched affine systems have been considered often in the literature via the hybrid dynamical paradigm [27]. The reader may refer to [3, 9, 28] for instance.
 40 The advantages of this framework relies on the possibility to account for the full continuous/discrete nature of such a class of systems. More especially, it allows to represent in a consistent and elegant manner periodic as well as aperiodic controllers. Hence, this direction can be beneficial for deriving a unified approach to cope with the time- and event-triggered switching control
 45 laws as for sampled-data systems. Indeed, several hybrid dynamical models have been considered to capture the particular class of sampled-data systems as explained for instance in [27], and have led to many relevant results as detailed in [29]. This represents the main motivation of this paper, i.e. enhance a hybrid controller for switched affine systems.

50 In the present paper, we follow the hybrid dynamical system paradigm provided in [27], generating both a periodic time-triggered control and an aperiodic event-triggered control for switched affine systems, without being based on a Lyapunov matrix-based mi-projection control strategy. We first provide a hybrid dynamical model of a controlled switching affine system, whose control
 55 input is required to be periodically updated, in the sense that the control input can be only modified at periodic sampling instants, driving to a periodic time-triggered controller. Then, we formulate an optimal control design problem expressed as a set of tractable matrix inequality conditions. The periodic time-triggered control law presents a simple structure, which is based on a so-

60 called free-matrices based control law and which differs from the well-known
 Lyapunov matrix-based min-projection control [9, 25, 30] used in this class of
 systems. This solution also provides a compact attractor of small size, which
 is proven to be Uniformly Globally Asymptotically Stable (UGAS). This en-
 65 sures that a given operating point is uniformly globally practically stable. In
 a second step, the previous model is extended in order to derive an aperiodic
 event-triggered control law, which includes a minimum dwell time constraint.
 This new hybrid dynamical model allows the controller to keep the same control
 action while no event are generated after a prescribed dwell time. A numerical
 example illustrates our contribution and shows the efficiency of our approach in
 70 the time- and event-triggered cases.

The paper is organized as follow. The problem formulation is stated in Sec-
 tion 2. The hybrid dynamical model for a time-triggered control is presented in
 Section 3, proposing a control design, by formulating an optimization problem.
 Moreover, the extension to an event-triggered control is given in Section 4. In
 75 Section 5 some numerical results illustrates the theoretical results. The paper
 ends with a conclusion section and draws some perspectives.

Notations: Throughout the paper, \mathbb{N} denotes the set of natural numbers,
 \mathbb{R} , the real numbers, $\mathbb{R}_{\geq 0}$ real positive numbers, \mathbb{R}^n the n -dimensional Euclidean
 space and $\mathbb{R}^{n \times m}$ the set of all real $n \times m$ matrices. The set composed by the
 80 first K positive integers, namely $\{1, 2, \dots, K\}$, is denoted by \mathbb{K} . For any n and
 m in \mathbb{N} , matrices I_n and $0_{n,m}$ denote the identity matrix of $\mathbb{R}^{n \times n}$ and the null
 matrix of $\mathbb{R}^{n \times m}$, respectively. When no confusion is possible, the subscripts
 of this matrix that precise the dimension, will be omitted. For any matrix M
 of $\mathbb{R}^{n \times n}$, the notation $M \succ 0$, ($M \prec 0$) means that M is symmetric positive
 85 (negative) definite and $\det(M)$ represents its determinant. Finally, we define Λ
 as the subset of $[0, 1]^{\text{Card}(\mathbb{K})}$ such that an element λ in Λ has its components, λ_i
 in $[0, 1]$ for all $i \in \mathbb{K}$ and and verifies $\sum_{i \in \mathbb{K}} \lambda_i = 1$.

2. Problem formulation

2.1. System data

Consider the switched affine system governed by the following dynamics:

$$\begin{aligned} \dot{z}(t) &= A_{\sigma(t)}z(t) + \mathcal{B}_{\sigma(t)}, \\ \sigma(t) &\in \mathbb{K}, \end{aligned} \quad \forall t \geq 0 \quad (1)$$

90 where $z(t) \in \mathbb{R}^n$ is the system state, and A_i and \mathcal{B}_i , for all i in \mathbb{K} are matrices
 of appropriate dimensions. The control input is the switching signal $\sigma(t)$ in \mathbb{K} .
 The two following assumptions on the implementation of the control law will be
 considered in the sequel:

Assumption 1 (Periodic time-triggered control). *There exists a sampling
 period $T > 0$ and an initial time t_0 (without loss of generality, we will take the*

convention $t_0 = 0$) such that the switching control input verifies :

$$\begin{cases} \sigma(t) = \sigma(t_k), & \forall t \in [t_k, t_{k+1}), \\ t_{k+1} = t_k + T, \end{cases} \quad \forall k \in \mathbb{N}. \quad (2)$$

Assumption 2 (Aperiodic event-triggered control). *There exists a minimum and a maximum dwell time $0 < T_m < T_M$, a function ϕ and an initial time $t_0 (= 0)$, such that the switching control input verifies :*

$$\begin{cases} \sigma(t) = \sigma(t_k), & \forall t \in [t_k, t_{k+1}), \\ t_{k+1} = \min_{t \in \mathbb{R}} \{t \in [t_k + T_m, t_k + T_M], \phi(\xi) \geq 0\}, \end{cases} \quad \forall k \in \mathbb{N}, \quad (3)$$

where function ϕ refers to the triggering rule to be defined that generates the events based on the available information, which denoted here as ξ .

This paper deals with the design of both periodic time- and an aperiodic event-triggered control law for the control input $\sigma(t)$, such that the solutions to switched affine system (1) converge globally and asymptotically to a neighborhood of a desired equilibrium given by $z_e \in \mathbb{R}^N$. As mentioned in the introduction, this desired equilibrium, z_e , is not necessarily an equilibrium of one or several modes of (1). The following definition and assumption that represent a sufficient condition for characterizing this equilibrium, are given next (see [16, 25]).

Definition 1. *Consider the set Ω_e given by*

$$\Omega_e := \{z_e \in \mathbb{R}^n, \exists \lambda \in \Lambda, A_\lambda z_e + \mathcal{B}_\lambda = 0\} \quad (4)$$

where $A_\lambda := \sum_{i \in \mathbb{K}} \lambda_i A_i$ and $\mathcal{B}_\lambda := \sum_{i \in \mathbb{K}} \lambda_i \mathcal{B}_i$.

Assumption 3. *The desired operating point, denoted as z_e in the remainder of the paper and its associated weighting vector, denoted as λ , belongs to Ω_e .*

It is worth noting that Ω_e does not contain all the acceptable functioning points as mentioned in [25]. For any vector z_e in Ω_e , we introduce the error variable $x(t) := z(t) - z_e$, where variable z is driven by system (1), giving rise to the following error dynamics

$$\begin{aligned} \dot{x}(t) &= A_{\sigma(t_k)} x + B_{\sigma(t_k)}, \\ \sigma(t_k) &\in \mathbb{K}, \end{aligned} \quad \forall t \in [t_k, t_{k+1}), \quad \forall k \in \mathbb{N}, \quad (5)$$

where matrices B_i stand for $A_i z_e + \mathcal{B}_i$, for all i in \mathbb{K} . Thus, from Assumption 3, the λ in Λ implies $B_\lambda = \sum_{i \in \mathbb{K}} \lambda_i B_i = 0$.

2.2. Control objectives

Even with a suitable control law, it is worth noting that systems (1) and (5) do not necessarily converge to z_e and 0, respectively, but to a neighborhood of them. This might be understood as a chattering effect around a sliding surface of a sampled-data sliding mode control law [31]. In the present paper, our objective is to study such systems using a hybrid dynamical system formulation and analysis as developed in [27]. This is formulated in the following statement:

Problem 1. *Consider system (1) with the periodic time-triggered control formulated in Assumption 1 or the event-triggered one mentioned in Assumption 2. For each case, the objectives of this paper are*

(P1) *To build a well-posed hybrid dynamical model.*

(P2) *To design a suitable control law, called free-matrix min-projection control.*

(P3) *To ensure that a neighborhood of the desired equilibrium z_e in Ω_e is uniformly globally asymptotic stable to the resulting closed-loop system.*

(P4) *To provide an optimal parametrization of the control law that minimizes the volume of that neighborhood.*

Objective (P1) remains in expressing switched affine system with a periodic or an aperiodic implementation, based on the hybrid dynamical system formulation considered in [27]. Contrary to the usual control law employed in the literature, i.e. Lyapunov matrix-based min projection control (see for instance [7, 25, 30]) our objective (P2) is to provide a relaxed structure for the control law inspired from the ones presented in [26, 32]. In order to prove the uniform global asymptotic stability of the system to the neighborhood of the equilibrium, objective (P3), the non smooth hybrid invariance principle from [33] will be used to characterize the neighborhood of the equilibrium thanks to a Lyapunov function for the hybrid system. Finally, an optimization problem will be formulated to reduce the size of this neighborhood following the problem presented in [25], fulfilling objective (P4). The novelty of this paper then, relies on the appropriate combination of these ingredients, considering time- and event-triggered control implementations.

3. Time-triggered control

3.1. Definition of a hybrid dynamical model

Considering (5), it is reasonable to model this system as a hybrid dynamical system, following the formalism given in [27], wherein continuous-time behavior is gathered in (5) and the discrete-time behavior is given by the jump of the control input σ from one mode to another one. A timer τ is included in the

hybrid model in order to consider the periodic implementation of the control law. Therefore, the overall dynamics are represented as follows:

$$\mathcal{H} : \begin{cases} \begin{bmatrix} \dot{x} \\ \dot{\tau} \\ \dot{\sigma} \end{bmatrix} = f(x, \tau, \sigma) & (x, \tau, \sigma) \in \mathcal{C}, \\ \begin{bmatrix} x^+ \\ \tau^+ \\ \sigma^+ \end{bmatrix} \in G(x, \tau, \sigma) & (x, \tau, \sigma) \in \mathcal{D}, \end{cases} \quad (6)$$

where $\sigma^+ \subset \mathbb{K}$ is the control law to be designed, $\tau \in \mathbb{R}$ is the timer that has to be constrained to live in the interval $[0, T]$. In the previous equation, f and G are (set-valued) maps that capture the continuous time dynamics as well as the switching logic. There are defined as follow:

$$\begin{aligned} f(x, \tau, \sigma) &:= \begin{bmatrix} A_\sigma x + B_\sigma \\ 1 \\ 0 \end{bmatrix} & (x, \tau, \sigma) \in \mathbb{H} := \mathbb{R}^n \times [0, T] \times \mathbb{K}, \\ G(x, \tau, \sigma) &:= \begin{bmatrix} x \\ 0 \\ u(x, \tau, \sigma) \end{bmatrix} & (x, \tau, \sigma) \in \mathbb{H}, \end{aligned} \quad (7)$$

where u is the control law to be designed.

The so-called “flow” and “jump” sets \mathcal{C} and \mathcal{D} , respectively, are given by

$$\mathcal{C} := \{(x, \tau, \sigma) : x \in \mathbb{R}^n, \tau \in [0, T], \sigma \in \mathbb{K}\}, \quad (8)$$

$$\mathcal{D} := \{(x, \tau, \sigma) : x \in \mathbb{R}^n, \tau = T, \sigma \in \mathbb{K}\}. \quad (9)$$

Note that the state of this hybrid model is composed of the state vector x of the original switched affine system, a timer τ that captures the elapsed time since the last control update and, the control input σ selected in the countable and bounded set \mathbb{K} . This model captures the whole dynamics of the sampled-data controlled system (see [29] for more details). Indeed, the system is allowed to flow only when $\tau \leq T$, which corresponds to the differential equation given by the map $f(x, \tau, \sigma)$ in \mathcal{H} . One can note that x evolves following the affine dynamic, timer τ increases as the time and the control input σ remains constant.

Likewise, the system is allowed to jump only when $\tau = T$, which corresponds to an update of the sampled-data switching control input as described by the jump map G in \mathcal{H} . During jumps, vector x remains constant, while timer τ is reset to 0 and control input σ is allowed to be modified according to the control law $u(x, \tau, \sigma)$. It is worth noting that the design of this hybrid model imposes that the control input σ is updated after T ordinary time.

This hybrid model description of \mathcal{H} presents good structural properties (see Proposition 1 below) and shows a periodic character of the jumps. Based on the previous considerations, the following proposition is stated.

Proposition 1. *System $\mathcal{H}(f, G, \mathcal{C}, \mathcal{D})$ is well-posed.*

Proof 1. *It is easy to see that hybrid system $\mathcal{H}(f, G, \mathcal{C}, \mathcal{D})$ verifies the following properties*

- \mathcal{C} and \mathcal{D} are closed sets in \mathbb{H} ;
- f is a continuous function, thus locally bounded and outer semi-continuous.
- 165 Moreover, it is convex for each $(x, \tau, \sigma) \in \mathcal{C}$;
- G is outer locally bounded and semi-continuous.

Therefore, it satisfies the basic hybrid conditions [27, Assumption 6.5] and following [27, Theorem 6.30], we can conclude that it is well posed.

Solutions to $\mathcal{H}(f, G, \mathcal{C}, \mathcal{D})$ are given on the hybrid time domain: $\text{dom}(x, \tau, \sigma) \subset \mathbb{R}_{\geq 0} \times \mathbb{N}$, such that,

$$\text{dom}(x, \tau, \sigma) = \bigcup_{k=0}^{\bar{k}-1} ([t_k, t_{k+1}], k), \quad (10)$$

with \bar{k} finite (being $\text{dom}(x, \tau, \sigma)$ a compact hybrid time domain) or infinite.

It is readily seen from system (5) that the following expression holds

$$\begin{bmatrix} \dot{x} \\ 0 \end{bmatrix} = \Gamma_\sigma \begin{bmatrix} x \\ 1 \end{bmatrix}, \quad \text{with} \quad \Gamma_\sigma := \begin{bmatrix} A_\sigma & B_\sigma \\ 0_{1,n} & 0 \end{bmatrix}, \quad (11)$$

so that the so-called hybrid arc (hybrid inclusion in [27]) defined in $I^k = [t_k, t_{k+1}]$ are given by

$$\begin{bmatrix} x_{k+1} \\ 1 \end{bmatrix} = e^{\Gamma_\sigma T} \begin{bmatrix} x_k \\ 1 \end{bmatrix}. \quad (12)$$

170 In the sequel, we will characterize some particular hybrid arcs that reach the origin just after a jump.

Definition 2. *Let us introduce the following set of hybrid arcs, defined as follows:*

$$\mathcal{E} = \left\{ (x, \tau, \sigma) \in \mathbb{H} \mid x = \begin{bmatrix} I & 0 \end{bmatrix} e^{\Gamma_\sigma \tau} \begin{bmatrix} 0 \\ 1 \end{bmatrix} \right\}. \quad (13)$$

In order to better understand the main motivation to introduce this set, let us note that, if $\tau = 0$, it is straightforward to see that the corresponding x is equal to zero. Hence, $x = \begin{bmatrix} I & 0 \end{bmatrix} e^{\Gamma_\sigma \tau} \begin{bmatrix} 0 \\ 1 \end{bmatrix}$ describes a solution that crosses the origin $(x, \tau, \sigma) = (0, 0, \sigma)$ and that flows from this point.

3.2. Definition of the attractor for time-triggered control

When considering system (5) with a T-periodic sampled-data control implementation of the input variable, σ , asymptotic stability to zero is in general not possible. However, only a practical stabilization of an operating point $x_e \in \Omega_e$ can be achieved. This can be also characterized by the asymptotic stability to a neighborhood of the origin. In this paper, we will consider this second formulation, where the attractor set will be defined through an appropriate candidate Lyapunov function, which is expressed using a positive definite matrix P to be defined latter on and is given by

$$V(x, \tau, \sigma) = \max \{W(x, \tau, \sigma) - 1, 0\}, \quad (14)$$

where W is a quadratic function of x , which is defined as follows,

$$W(x, \tau, \sigma) := \begin{bmatrix} x \\ 1 \end{bmatrix}^\top \mathcal{P}(\tau, \sigma) \begin{bmatrix} x \\ 1 \end{bmatrix}. \quad (15)$$

The function \mathcal{P} is a matrix that depends on the timer τ and on the active mode, σ . Several ways of constructing such timer-dependent functions have already been considered and the reader may refer to [34] to see some other examples. In this paper, we want to extend the formulation provided in [27] for periodic sampled-data control systems. This corresponds to the following definition

$$\begin{aligned} \mathcal{P}(\tau, \sigma) &= e^{-\Gamma_\sigma^\top \tau} \begin{bmatrix} P & h \\ h^\top & h^\top P^{-1} h \end{bmatrix} e^{-\Gamma_\sigma \tau} \\ &= e^{-\Gamma_\sigma^\top \tau} \begin{bmatrix} P \\ h^\top \end{bmatrix} P^{-1} \begin{bmatrix} P & h \end{bmatrix} e^{-\Gamma_\sigma \tau}, \end{aligned} \quad (16)$$

where matrices Γ_i , $i \in \mathbb{K}$ has been defined in (11). From the last expression, it is clear that the positive definiteness of P ensures in the previous expression that \mathcal{P} is positive definite and h is a vector that allows to shift the center of the level set. We are now in position to define the compact attractor, which is characterized as follows:

$$\mathcal{A} := \{(x, \tau, \sigma) \in \mathcal{C} \cup \mathcal{D} \mid V(x, \tau, \sigma) = 0\}. \quad (17)$$

This attractor refers to the elements of \mathbb{H} , that verify $W(x, \tau, \sigma) \leq 1$. It is worth noting that this set is described in an extended space composed not only by the system state x , but also by the timer τ and the active mode σ .

180 It is easy to see that V is continuous in $\mathcal{C} \cup \mathcal{D}$ and locally Lipschitz near each point in $\mathcal{C} \setminus \mathcal{A}$. Moreover, V is positive definite with respect to \mathcal{A} in $\mathcal{C} \cup \mathcal{D}$ and radially unbounded.

185 Note that the minimum of W with respect to x is not necessarily reached when (x, τ, σ) is equal to $(0, 0, \sigma)$. This is due to the introduction of parameter h , which allows shifting this minimum to another location. In order to achieve the control objectives, which means that the solutions are ensured to converge to a neighborhood of the origin, one has to guarantee that $(0, 0, \sigma)$ belongs to \mathcal{A} . More generally, regarding the definition of \mathcal{E} in (13), it will be required that \mathcal{E} is included in the attractor \mathcal{A} , to state that the origin is included in the attractor.

190 **Remark 1.** Note that function \mathcal{W} is a relatively simple quadratic function,
 whose center is shifted to the position defined by vector h . More involved
 functions can be found in the literature of switched affine systems, as for instance
 in [35], where the Lyapunov matrix P is allowed to depend on the active mode.
 This is not considered in this paper for the sake of simplicity. Indeed, our
 195 objective is more to focus on the hybrid framework and on the extension to the
 design of an event-triggered controller developed in the next section. \lrcorner

3.3. Design of an efficient switching control law

Once the Objective (P1) is fulfilled by the hybrid dynamical model given
 in \mathcal{H} , (6), we propose, in this section, a novel stabilization based on a relaxed
 200 control law, which notably differs from the classical Lyapunov matrix-based
 min-projection control developed in [7, 25, 30], among others. This is stated in
 the following theorem.

Theorem 1. For a given z_e in Ω_e and a given $T \in \mathbb{R}_{\geq 0}$, assume that matrices
 $P \in \mathbb{R}^{n \times n} \succ 0$, $h \in \mathbb{R}^n$, $N_i = N_i^\top \in \mathbb{R}^{(n+1) \times (n+1)}$, for all $i \in \mathbb{K}$ and parameter
 $0 < \mu < 1$ are the solution to the optimization problem

$$\min_{P, h, N_i, \mu} -\log(\det(P)), \quad (18)$$

$$\text{s.t. } P \succ 0, \quad (19)$$

$$\Phi_i(T) = \begin{bmatrix} \Psi_i(T) + N_\lambda - N_i - \begin{bmatrix} 0 & 0 \\ * & \mu \end{bmatrix} & \mu \begin{bmatrix} P \\ h^\top \end{bmatrix} \\ * & -\mu P \end{bmatrix} \prec 0, \quad \forall i \in \mathbb{K}, \quad (20)$$

$$\Theta_\lambda(T) = \begin{bmatrix} 0 \\ 1 \end{bmatrix}^\top \Psi_\lambda(T) \begin{bmatrix} 0 \\ 1 \end{bmatrix} \succeq 0, \quad (21)$$

where $\lambda \in \Lambda$ is related to z_e satisfying Assumption 3 and

$$\Psi_i(T) := e^{\Gamma_i^\top T} \begin{bmatrix} P & h \\ h^\top & 0 \end{bmatrix} e^{\Gamma_i T} - \begin{bmatrix} P & h \\ h^\top & 0 \end{bmatrix}. \quad (22)$$

$$N_\lambda := \sum_{i \in \mathbb{K}} \lambda_i N_i \quad \text{and} \quad \Psi_\lambda(T) := \sum_{i \in \mathbb{K}} \lambda_i \Psi_i(T).$$

Then, the following control law, given by

$$u(x, \tau, \sigma) = \underset{j \in \mathbb{K}}{\operatorname{argmin}} \begin{bmatrix} x \\ 1 \end{bmatrix}^\top N_j \begin{bmatrix} x \\ 1 \end{bmatrix} \quad (23)$$

with $x := z - z_e$ ensures that the following statements hold for hybrid system (6):

(i) \mathcal{A} defined in (17) is UGAS;

205 (ii) \mathcal{E} defined in (13) is included in \mathcal{A} .

□

Remark 2. The optimization problem given in Theorem 1 is, as stated, a bilinear matrix inequality, which is known to be non-convex. However, the problem can be easily avoided by performing a line-search routine for $\mu \in (0, 1)$ and by noting that the resulting problem has become linear with respect to the decision variables. Note that this procedure was already adopted in [25].

┘

Proof 2. For a given sampling period, T , let us consider a solution to the optimization described in Theorem 1. That is parameter $\mu \in (0, 1)$ and matrices
215 $P \succ 0 \in \mathbb{R}^{n \times n}$, $h \in \mathbb{R}^n$, $N_i = N_i^\top \in \mathbb{R}^{(n+1) \times (n+1)}$ with $i \in \mathbb{K}$ verify problem (18)-(21). In the sequel, the proof of items (i) and (ii) will be considered successively.

Proof of (i): The proof of item (i) relies on the application of [33, Theorem 1]. Let us first note that the candidate Lyapunov function, V (14) is locally
220 Lipschitz, radially unbounded and verifies, by definition $V(x, \tau, \sigma) = 0$, for all (x, τ, σ) in \mathcal{A} and strictly positive otherwise as shown in equation (16), where matrix P is assumed to be positive definite.

The next step of the proof is to ensure that the derivative of V along flows outside of \mathcal{A} is non positive (or more precisely in this case, equal to zero). More formally, the objective is to show

$$\langle \nabla V(x, \tau, \sigma), f(x, \sigma) \rangle \leq 0, \quad \forall (x, \tau, \sigma) \in \mathcal{C} \setminus \mathcal{A}. \quad (24)$$

For any $(x, \tau, \sigma) \in \mathcal{C} \setminus \mathcal{A}$, it is clear, from its definition, that $V(x, \tau, \sigma) = W(x, \tau, \sigma) - 1$ and we get that

$$\begin{aligned} \langle \nabla V(x, \tau, \sigma), f(x, \sigma) \rangle &= \begin{bmatrix} x \\ 1 \end{bmatrix}^\top \left(\dot{\tau} \frac{\partial}{\partial \tau} \mathcal{P}(\tau, \sigma) + \dot{\sigma} \frac{\partial}{\partial \sigma} \mathcal{P}(\tau, \sigma) \right) \begin{bmatrix} x \\ 1 \end{bmatrix} + 2 \begin{bmatrix} x \\ 1 \end{bmatrix}^\top \mathcal{P}(\tau, \sigma) \begin{bmatrix} \dot{x} \\ 0 \end{bmatrix} \\ &= \begin{bmatrix} x \\ 1 \end{bmatrix}^\top \left(\frac{\partial}{\partial \tau} \mathcal{P}(\tau, \sigma) + \text{He}(\mathcal{P}(\tau, \sigma) \Gamma_\sigma) \right) \begin{bmatrix} x \\ 1 \end{bmatrix} = 0, \end{aligned}$$

which is guaranteed by the construction of \mathcal{P} in (16), and ensures condition (24). Let us now the second stability condition from [33, Theorem 1], that is

$$\Delta V(x, \tau, \sigma) := \max_{g \in G(x, \tau, \sigma) \cap (\mathcal{C} \cup \mathcal{D})} V(g) - V(x, \tau, \sigma) < 0, \quad \forall (x, \tau, \sigma) \in \mathcal{D} \setminus \mathcal{A}. \quad (25)$$

Again, consider any (x, τ, σ) in $\mathcal{D} \setminus \mathcal{A}$, such that $V(x, \tau, \sigma) = W(x, \tau, \sigma) - 1$ and any g in $G(x, \tau, \sigma) \cap (\mathcal{C} \cup \mathcal{D})$. Since (x, τ, σ) is in $\mathcal{D} \setminus \mathcal{A}$, then $\tau = T$. Moreover, since g is in $G(x, \tau, \sigma) \cap (\mathcal{C} \cup \mathcal{D})$, then $g = (x, 0, \sigma^+)$ where σ^+ belongs to $u(x)$. If $(x, 0, \sigma^+)$ belongs to \mathcal{A} , then $V(x, 0, \sigma^+) - V(x, T, \sigma) = -V(x, T, \sigma) < 0$. Otherwise we have

$$\begin{aligned} V(x, 0, \sigma^+) - V(x, T, \sigma) &= W(x^+, 0, \sigma^+) - W(x, T, \sigma) \\ &= \begin{bmatrix} x \\ 1 \end{bmatrix}^\top (\mathcal{P}(0, \sigma^+) - \mathcal{P}(T, \sigma)) \begin{bmatrix} x \\ 1 \end{bmatrix} \\ &= \begin{bmatrix} x \\ 1 \end{bmatrix}^\top \left(\begin{bmatrix} P & h \\ h^\top & h^\top P^{-1} h \end{bmatrix} - e^{-\Gamma_\sigma^\top T} \begin{bmatrix} P & h \\ h^\top & h^\top P^{-1} h \end{bmatrix} e^{-\Gamma_\sigma T} \right) \begin{bmatrix} x \\ 1 \end{bmatrix} \\ &= \begin{bmatrix} x \\ 1 \end{bmatrix}^\top \left(\begin{bmatrix} P & h \\ h^\top & 0 \end{bmatrix} - e^{-\Gamma_\sigma^\top T} \begin{bmatrix} P & h \\ h^\top & 0 \end{bmatrix} e^{-\Gamma_\sigma T} \right) \begin{bmatrix} x \\ 1 \end{bmatrix}. \end{aligned}$$

This last simplification comes from the fact that the last diagonal component of $e^{-\Gamma_\sigma T}$ is 1. Therefore, we can express the previous equation thanks to the matrices Ψ_i 's defined in (22) as follows

$$V(x, 0, \sigma^+) - V(x, T, \sigma) = \left(e^{-\Gamma_\sigma T} \begin{bmatrix} x \\ 1 \end{bmatrix} \right)^\top \Psi_\sigma(T) \left(e^{-\Gamma_\sigma T} \begin{bmatrix} x \\ 1 \end{bmatrix} \right). \quad (26)$$

For the sake of simplicity, we will use the following notation along the proof,

$$\begin{bmatrix} \chi \\ 1 \end{bmatrix} = e^{-\Gamma_\sigma T} \begin{bmatrix} x \\ 1 \end{bmatrix}. \quad (27)$$

Notice that, in this definition, the vector χ depends on both the sampling period T and on the active mode σ . This dependence is not specified in this notation to avoid heavy notations.

We also note that this new notation is of high importance since it corresponds to the state of the switched affine system just after the jump. Hence, according to (12), this can be formalized as follows

$$\sigma \in \underset{j \in \mathbb{K}}{\operatorname{argmin}} \begin{bmatrix} \chi \\ 1 \end{bmatrix}^\top N_j \begin{bmatrix} \chi \\ 1 \end{bmatrix}.$$

This implies that inequality

$$\begin{bmatrix} \chi \\ 1 \end{bmatrix}^\top (N_j - N_\sigma) \begin{bmatrix} \chi \\ 1 \end{bmatrix} \geq 0,$$

holds for any $j \in \mathbb{K}$. Therefore, for any convex combination for the particular case λ in Λ , we have

$$\Sigma_\sigma(x, T, \sigma) := \begin{bmatrix} \chi \\ 1 \end{bmatrix}^\top (N_\lambda - N_\sigma) \begin{bmatrix} \chi \\ 1 \end{bmatrix} \geq 0. \quad (28)$$

The previous expression allows to introduce the condition that σ is the active node. Let us now specify that (x, T, σ) is in $\mathcal{D} \setminus \mathcal{A}$. From the definition of \mathcal{A} , this means that $V(x, T, \sigma) > 0$ and

$$\begin{aligned} 0 < W(x, T, \sigma) - 1 &= \begin{bmatrix} x \\ 1 \end{bmatrix}^\top \mathcal{P}(T, \sigma) \begin{bmatrix} x \\ 1 \end{bmatrix} - 1 \\ &= \begin{bmatrix} \chi \\ 1 \end{bmatrix}^\top \begin{bmatrix} P & h \\ h^\top & h^\top P^{-1} h - 1 \end{bmatrix} \begin{bmatrix} \chi \\ 1 \end{bmatrix}, \end{aligned}$$

where we have employed (27) to enforce the use of notation χ . Therefore, (25) is verified, if we can prove that inequality

$$\begin{bmatrix} \chi \\ 1 \end{bmatrix}^\top \Psi_i(T) \begin{bmatrix} \chi \\ 1 \end{bmatrix} < 0$$

holds for all (x, τ, σ) in $\mathcal{D} \setminus \mathcal{A}$ such that

$$\begin{aligned} & \begin{bmatrix} \chi \\ 1 \end{bmatrix}^\top \begin{bmatrix} P & h \\ h^\top & h^\top P^{-1} h - 1 \end{bmatrix} \begin{bmatrix} \chi \\ 1 \end{bmatrix} \geq 0 \\ \text{and} \quad & \begin{bmatrix} \chi \\ 1 \end{bmatrix}^\top (N_\lambda - N_\sigma) \begin{bmatrix} \chi \\ 1 \end{bmatrix} \geq 0, \end{aligned}$$

where we recall that vector χ , defined in (27), depends explicitly on (x, τ, σ) . Using two successive S -procedures, this problem is recast into the existence of a parameter $\mu > 0$, such that,

$$\Psi_i(T) + N_\lambda - N_i + \mu \begin{bmatrix} P & h \\ h^\top & h^\top P^{-1} h - 1 \end{bmatrix} \prec 0, \quad i \in \mathbb{K}. \quad (29)$$

By noting that matrix $\begin{bmatrix} P & h \\ h^\top & h^\top P^{-1} h - 1 \end{bmatrix}$ can be rewritten as $\begin{bmatrix} P \\ h^\top \end{bmatrix} P^{-1} \begin{bmatrix} P \\ h^\top \end{bmatrix}^\top$, such that, the application of the Schur complement to this term leads to condition (20). It can then, be concluded that if (20) is satisfied, then condition (25) is also verified.

In order to complete the proof, the assumption of [33, Theorem 1], consisting in the satisfaction of $G(\mathcal{A} \cap \mathcal{D}) \subset \mathcal{A}$ has to be included. This condition consists in proving that \mathcal{A} is invariant. Let us first note that in the proof of (24), we prove that V is constant in $\mathcal{C} \cap \mathcal{A}$. Then, let us consider (x, τ, σ) in $\mathcal{D} \cap \mathcal{A}$. We have seen in the previous calculations that, if inequality (20) holds, then we have

$$\begin{aligned} & \left(e^{-\Gamma_\sigma T} \begin{bmatrix} x \\ 1 \end{bmatrix} \right)^\top \left(\Psi_i(T) + N_\lambda - N_i + \mu \begin{bmatrix} P & h \\ h^\top & h^\top P^{-1} h - 1 \end{bmatrix} \right) \left(e^{-\Gamma_\sigma T} \begin{bmatrix} x \\ 1 \end{bmatrix} \right) \\ & = W(x, 0, \sigma^+) - W(x, T, \sigma) + \mu(W(x, T, \sigma) - 1) + \Sigma_\sigma < 0, \end{aligned}$$

where Σ_σ is defined in (28) and is a positive quantity. The previous expression can be rewritten as follows

$$W(x, 0, \sigma^+) - 1 < (1 - \mu)(W(x, T, \sigma) - 1) - \Sigma_\sigma \leq (1 - \mu)(W(x, T, \sigma) - 1).$$

Therefore, since $\mu \in (0, 1)$ and $(x, T, \sigma) \in \mathcal{A}$, ensures that $W(x, 0, \sigma^+) - 1$ is negative, such that, $V(x, 0, \sigma^+)$ is zero, which was to be proven. The last

step of the proof is to ensure that no complete solution, that are not in \mathcal{A} , keeps constant, this means that there is no complete solution such that

$$V(x(t, j), \tau(t, j), \sigma(t, j)) = V(x(0, 0), \tau(0, 0), \sigma(0, 0)) \neq 0,$$

230 for all $(t, j) \in \text{dom}(x, \tau, \sigma)$. This is ensured by the facts that condition (20) is a strict inequality and that jumps are forced to occurs after T ordinary time. Therefore, by application of [33, Theorem 1], attractor \mathcal{A} is UGAS for hybrid system \mathcal{H} .

Proof of (ii): The objective here is to prove that the particular solutions in \mathcal{E} are in the interior of \mathcal{A} . Recall that \mathcal{E} contains the solutions that reach the origin (in x) right after a jump. Formally, this means that inequality

$$\left(e^{\Gamma_\sigma \tau} \begin{bmatrix} 0 \\ 1 \end{bmatrix} \right)^\top \mathcal{P}(\tau, \sigma) \left(e^{\Gamma_\sigma \tau} \begin{bmatrix} 0 \\ 1 \end{bmatrix} \right) = \begin{bmatrix} 0 \\ 1 \end{bmatrix}^\top \mathcal{P}(0, \sigma) \begin{bmatrix} 0 \\ 1 \end{bmatrix} = h^\top P^{-1} h \leq 1,$$

holds for any (τ, σ) in $[0, T] \times \mathbb{K}$. To proceed with this proof, let us compute the linear combination of (29) (which is equivalent to LMI (20)), weighted by λ . This yields

$$\sum_{i \in \mathbb{K}} \lambda_i \left(\Psi_i(T) + N_\lambda - N_i + \mu \begin{bmatrix} P & h \\ h^\top & h^\top P^{-1} h - 1 \end{bmatrix} \right) \prec 0.$$

Using the condition $\sum_{i \in \mathbb{K}} \lambda_i = 1$ and the fact that $\sum_{i \in \mathbb{K}} \lambda_i N_i = N_\lambda$, the previous inequality leads to

$$\sum_{i \in \mathbb{K}} \lambda_i \Psi_i(T) + \mu \begin{bmatrix} P & h \\ h^\top & h^\top P^{-1} h - 1 \end{bmatrix} \prec 0.$$

Pre- and post-multiplying this inequality by the vector $\begin{bmatrix} 0 \\ 1 \end{bmatrix}^\top$ and its transpose, respectively leads to

$$\begin{bmatrix} 0 \\ 1 \end{bmatrix}^\top \sum_{i \in \mathbb{K}} \lambda_i \Psi_i(T) \begin{bmatrix} 0 \\ 1 \end{bmatrix} + \mu(h^\top P^{-1} h - 1) < 0.$$

235 From condition (21), the first term of the previous inequality is positive. This necessarily implies that $h^\top P^{-1} h - 1$ is negative, which was to be demonstrated.

The hybrid dynamical model given in (6)–(7) together with the solution of the optimization problem given in Theorem 1 satisfy all items of Problem 1.

Remark 3. The optimization problem formulated in Theorem 1 consists in the minimization of a characteristic of attractor \mathcal{A} . Indeed, maximizing $\log(\det(P))$ refers to the minimization of the volume of the ellipse defined by the positive definite matrix P . \lrcorner

4. Event-triggered control

4.1. Definition of a new hybrid dynamical model

In this section, we want to relax the constraint on the periodic update of the switching control law, by considering Assumption 2. This relaxation allows that the trajectories reach a region around a given equilibrium $z_e \in \Omega_e$ with less control updates, than using the periodic-switching control considered in Assumption 1. To do so, let us represent the overall dynamics as follows:

$$\tilde{\mathcal{H}} : \begin{cases} \begin{bmatrix} \dot{x} \\ \dot{\tau} \\ \dot{\sigma} \end{bmatrix} = f(x, \tau, \sigma) & (x, \tau, \sigma) \in \tilde{\mathcal{C}}, \\ \begin{bmatrix} x^+ \\ \tau^+ \\ \sigma^+ \end{bmatrix} \in G(x, \tau, \sigma) & (x, \tau, \sigma) \in \tilde{\mathcal{D}}, \end{cases} \quad (30)$$

where we use the same three components and the same maps f and G to express the state variables as in the periodic time-triggered implementation considered in Section 3.1. However, in order to enforce the event-triggered control, the definition of the jump and flow sets $\tilde{\mathcal{C}}$ and $\tilde{\mathcal{D}}$ have to be modified. Let us first recall maps f and G that capture the new features of the system, as well as, the switching logic. For a sufficiently large positive real T_M , they are now defined as follows:

$$\begin{aligned} f(x, \tau, \sigma) &:= \begin{bmatrix} A_\sigma x + B_\sigma \\ 1 \\ 0 \end{bmatrix} & (x, \tau, \sigma) \in \tilde{\mathbb{H}} := \mathbb{R}^n \times [0, T_M] \times \mathbb{K}, \\ G(x, \tau, \sigma) &:= \begin{bmatrix} x \\ 0 \\ u(x, \tau, \sigma) \end{bmatrix} & (x, \tau, \sigma) \in \tilde{\mathbb{H}}, \end{aligned} \quad (31)$$

where u is again the control law to be defined.

The timer presents the same role as in the previous section, i.e. keeping track of the elapsed time since the last jump. Timer τ is now enforced to lie in the interval $[0, T_M]$, so that T_M can be seen as a maximum dwell time parameter,

which can be selected arbitrarily. Likewise, a minimum dwell time parameter $T_m \in [0, T_M]$ has now to be included. The new flow and jump sets $\tilde{\mathcal{C}}$ and $\tilde{\mathcal{D}}$, respectively, are now given by

$$\tilde{\mathcal{C}} := (\mathcal{C}_{T_m} \cup \mathcal{C}_e) \cap \mathcal{C}_{T_M}, \quad (32)$$

$$\tilde{\mathcal{D}} := (\mathcal{D}_{T_m} \cap \mathcal{D}_e) \cup \mathcal{D}_{T_M}, \quad (33)$$

where

$$\text{minimum dwell time } \begin{cases} \mathcal{C}_{T_m} := \{(x, \tau, \sigma) \in \tilde{\mathbb{H}} : \tau \leq T_m\}, \\ \mathcal{D}_{T_m} := \{(x, \tau, \sigma) \in \tilde{\mathbb{H}} : \tau \geq T_m\}, \end{cases}$$

$$\text{maximum dwell time } \begin{cases} \mathcal{C}_{T_M} := \{(x, \tau, \sigma) \in \tilde{\mathbb{H}} : \tau \leq T_M\}, \\ \mathcal{D}_{T_M} := \{(x, \tau, \sigma) \in \tilde{\mathbb{H}} : \tau = T_M\}, \end{cases}$$

$$\text{Event-triggering rule } \begin{cases} \mathcal{C}_e := \{(x, \tau, \sigma) \in \tilde{\mathbb{H}}, \tau \in [T_m, T_M], \phi(x, \tau, \sigma) \leq 0\}, \\ \mathcal{D}_e := \{(x, \tau, \sigma) \in \tilde{\mathbb{H}}, \tau \in [T_m, T_M], \phi(x, \tau, \sigma) = 0\}, \end{cases}$$

where $\phi : \tilde{\mathbb{H}} \rightarrow \mathbb{R}$ is the triggering function, which allows the controller to decide whether or not an event occurs. For the sake of consistency, the definition of this function will be given in the sequel. The following constraint on ϕ is imposed

$$\phi(x, T_m, \sigma) \leq 0, \quad \forall (x, \sigma) \in \mathbb{R}^n \times \mathbb{K}. \quad (34)$$

We also note that some elements of $\tilde{\mathbb{H}}$ are disregarded. Indeed, the element of $\{(x, \tau, \sigma) \in \tilde{\mathbb{H}}, \tau \in [T_m, T_M], \phi(x, \tau, \sigma) > 0\}$ are not relevant to consider in this study.

Sets $\tilde{\mathcal{C}}$ and $\tilde{\mathcal{D}}$ are subspaces of $\tilde{\mathbb{H}}$. The system has to be understood as follows. According to (32), the system is constrained to flow

- when the timer is lower than the minimum dwell time T_m , as depicted in Figure 1 by the yellow area.
- when the timer is greater than T_m , and the triggering condition $\phi(x, \tau, \sigma) \leq 0$ remains satisfied and if timer τ remains lower than the maximum dwell time T_M , as depicted in Figure 1 by the red area.

Reversely, according to (33), the system is constrained to jump

- when the timer is greater than the minimum dwell time T_m and when $\phi(x, \tau, \sigma) = 0$ becomes true, i.e. the bold blue line in Figure 1.
- when the timer becomes equal to the maximum dwell time T_M , while the triggering condition $\phi(x, \tau, \sigma) \leq 0$ has not been violated, i.e. the bold green line in Figure 1.

Figure 1 also illustrates that condition $\phi(x, T_m, \sigma) < 0$ ensures that maximum solutions are complete, since the solutions to the system have to enter in the red area and have then to enter in the jump set.

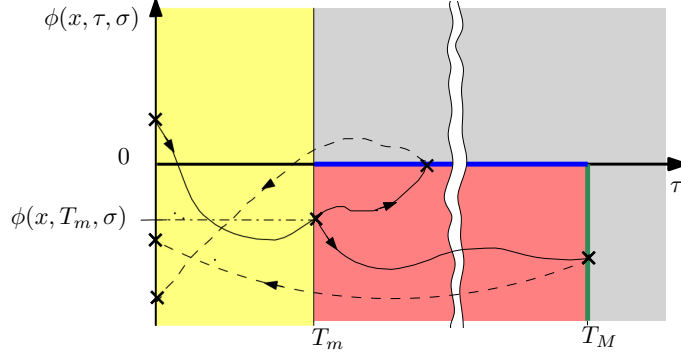


Figure 1: Illustration of the jump and flow sets in the plan $\tau, \phi(x, \tau, \sigma)$ and two potential solutions to hybrid system $\tilde{\mathcal{H}}(f, G, \tilde{\mathcal{C}}, \tilde{\mathcal{D}})$.

As for the periodic time-triggered control case, one has first to prove the well-posedness of this new hybrid dynamical system. This is done in the next proposition.

Proposition 2. *System $\tilde{\mathcal{H}}(f, G, \tilde{\mathcal{C}}, \tilde{\mathcal{D}})$ is well posed.*

The proof is similar to the one of Proposition 1 and is therefore omitted.

The solutions of $\tilde{\mathcal{H}}$ are given in $\text{dom}(x, \tau, \sigma)$ provided in (10). As for the time-triggered control implementation, let us now define the set of the particular arcs starting in the origin for $\tilde{\mathcal{H}}$, which are similar to \mathcal{E} for \mathcal{H} .

Definition 3. *Let us introduce the following set of hybrid arcs, defined as follows:*

$$\tilde{\mathcal{E}} = \left\{ \begin{bmatrix} x \\ \tau \\ \sigma \end{bmatrix} \in \mathbb{R}^n \times [0, T_m] \times \mathbb{K} \mid x = \begin{bmatrix} I & 0 \end{bmatrix} e^{\Gamma \sigma \tau} \begin{bmatrix} 0 \\ 1 \end{bmatrix} \right\}. \quad (35)$$

The set has the same definition as in the periodic case. The only difference is that it only contains the trajectories of the system that are located at $x = 0$ after a jump and that flows until the minimum dwell time T_m is reached. Of course, thanks to the event-triggered control law, these trajectories may continue flowing after the minimum dwell time. However, this set is only defined to understand that the trajectories that starts at $x = 0$ after a jump stay close enough to the equilibrium and to the attractor that is defined in the next section.

4.2. Definition of the attractor for event-triggered control

The attractor related to system (5) with an aperiodic sampled-data control implementation, is defined with the same candidate Lyapunov function as for the periodic time-triggered case, i.e.

$$V(x, \tau, \sigma) = \max \{W(x, \tau, \sigma) - 1, 0\}, \quad (36)$$

where W is defined in (15) where we also keep the same definition for $\mathcal{P}(\tau, \sigma)$ given in (16). We recall that matrices Γ_i have been given in (11) and that $\mathcal{P} \succ 0$, which is directly deduced from the definite-positiveness of P . Now, we can define the new compact attractor as follows:

$$\tilde{\mathcal{A}} := \left\{ (x, \tau, \sigma) \in \tilde{\mathcal{C}} \cup \tilde{\mathcal{D}}, \quad V(x, \tau, \sigma) = 0 \right\}. \quad (37)$$

In other words, this attractor is the subset of $\tilde{\mathbb{H}}$, where the solutions to $\tilde{\mathcal{H}}$ satisfy $W(x, \tau, \sigma) \leq 1$ and $\tau < T_M$. We are now in position to state the next theorem.

Theorem 2. For a given $z_e \in \Omega_e$ and given $T_m, T_M \in \mathbb{R}$, such that, $0 < T_m < T_M$, assume that matrices $P \in \mathbb{R}^{n \times n}$, $M = M^\top \in \mathbb{R}^{(n+1) \times (n+1)}$, $h \in \mathbb{R}^n$, $N_i = N_i^\top \in \mathbb{R}^{(n+1) \times (n+1)}$ and parameters $\mu \in (0, 1)$ and are the solution to the optimization problem

$$\min_{P, M, h, N_i, \mu} -\log(\det(P)), \quad (38)$$

$$\text{s.t. } P \succ 0, \quad M \succ 0, \quad \Theta_\lambda(T_m) \succeq 0, \quad (39)$$

$$\begin{aligned} & \begin{bmatrix} \Psi_i(T_m) + (N_\lambda - N_i) + e^{\Gamma_i^\top T_m} M e^{\Gamma_i T_m} - \begin{bmatrix} 0 & 0 \\ * & \mu \end{bmatrix} & \mu \begin{bmatrix} P \\ h^\top \end{bmatrix} \\ * & -\mu P \end{bmatrix} \prec 0, \\ & \forall i \in \mathbb{K}, \end{aligned} \quad (40)$$

where $\Psi_i(T_m)$ and $\Theta_\lambda(T_m)$ is given in (22) and (21), respectively, with T_m replacing T and with $\lambda \in \Lambda$ is related to z_e satisfying Assumption 3. Then, the following control law, given by

$$u(x, \tau, \sigma) \in \operatorname{argmin}_{j \in \mathbb{K}} \begin{bmatrix} x \\ 1 \end{bmatrix}^\top N_j \begin{bmatrix} x \\ 1 \end{bmatrix} \quad (41)$$

with $x := z - z_e$ together with the event-triggering rule

$$\phi(x, \tau, \sigma) = \begin{bmatrix} x \\ 1 \end{bmatrix}^\top \left(\mathcal{P}(0, \sigma) - e^{\Gamma_\sigma^\top (T_m - \tau)} (\mathcal{P}(0, \sigma) + M) e^{\Gamma_\sigma (T_m - \tau)} \right) \begin{bmatrix} x \\ 1 \end{bmatrix} \quad (42)$$

ensures that the following statements hold for hybrid system (30)–(31):

- 290 (i) Attractor $\tilde{\mathcal{A}}$ defined in (37) is UGAS;

(ii) Set $\tilde{\mathcal{E}}$ defined in (35) is included in attractor $\tilde{\mathcal{A}}$.

□

Proof 3. Consider the solution of the optimization described in Theorem 2, for a given minimum dwell time, T_m and a maximum dwell time, T_M , which is selected arbitrarily with the only constraint that $T_M > T_m$. Then, we proceed with the proof of items (i) and (ii).

Proof of (i): The proof of item (i) relies on the application of [33, Theorem 1]. It is easy to see that V presents, as in the previous section, the properties of continuity in $\tilde{\mathcal{C}} \cup \tilde{\mathcal{D}}$, locally Lipschitz near each point in $\tilde{\mathcal{C}} \setminus \tilde{\mathcal{A}}$, positive definiteness with respect to $\tilde{\mathcal{A}}$ in $\tilde{\mathcal{C}} \cup \tilde{\mathcal{D}}$ and radially unbounded.

Now, the next step of the proof is to ensure

$$\langle \nabla V(x, \tau, \sigma), f(x, \sigma) \rangle \leq 0, \quad \forall (x, \tau, \sigma) \in \tilde{\mathcal{C}} \setminus \tilde{\mathcal{A}}. \quad (43)$$

From definition of V given in (36) we get that

$$\begin{aligned} & \langle \nabla V(x, \tau, \sigma), f(x, \tau, \sigma) \rangle \\ &= \begin{bmatrix} x \\ 1 \end{bmatrix}^\top \left(\dot{\tau} \frac{\partial}{\partial \tau} \mathcal{P}(\tau, \sigma) + \dot{\sigma} \frac{\partial}{\partial \sigma} \mathcal{P}(\tau, \sigma) \right) \begin{bmatrix} x \\ 1 \end{bmatrix} + 2 \begin{bmatrix} x \\ 1 \end{bmatrix}^\top \mathcal{P}(\tau, \sigma) \begin{bmatrix} \dot{x} \\ 0 \end{bmatrix} \\ &= \begin{bmatrix} x \\ 1 \end{bmatrix}^\top (1 - \dot{\tau}) \text{He}(\mathcal{P}(\tau, \sigma) \Gamma_\sigma) \begin{bmatrix} x \\ 1 \end{bmatrix} = 0, \end{aligned} \quad (44)$$

which is guaranteed by the positive definiteness of V in $\tilde{\mathcal{C}} \setminus \tilde{\mathcal{A}}$. The next step consists in establishing the following condition during jumps

$$\Delta V(x, \tau, \sigma) := \max_{\tilde{g} \in G(x, \tau, \sigma) \cap (\tilde{\mathcal{C}} \cup \tilde{\mathcal{D}})} V(\tilde{g}) - V(x, \tau, \sigma) < 0, \quad \forall (x, \tau, \sigma) \in \tilde{\mathcal{D}} \setminus \tilde{\mathcal{A}}. \quad (45)$$

Let us first note that, if the first term of the right hand side is 0 (i.e. $\tilde{g} \in \tilde{\mathcal{A}}$), then, the negativity of the previous equation is trivially satisfied. If not, we have,

from the definition of V in (36),

$$\begin{aligned}
\Delta V(x, \tau, \sigma) &= W(x^+, 0, \sigma^+) - W(x, T, \sigma) \\
&= \begin{bmatrix} x \\ 1 \end{bmatrix}^\top \left(\mathcal{P}(0, \sigma) - e^{-\Gamma_\sigma^\top \tau} \mathcal{P}(0, \sigma) e^{-\Gamma_\sigma \tau} \right) \begin{bmatrix} x \\ 1 \end{bmatrix} \\
&= \begin{bmatrix} x \\ 1 \end{bmatrix}^\top e^{-\Gamma_\sigma^\top \tau} \left(e^{\Gamma_\sigma^\top T_m} (\mathcal{P}(0, \sigma) + M) e^{\Gamma_\sigma T_m} - \mathcal{P}(0, \sigma) \right) e^{-\Gamma_\sigma \tau} \begin{bmatrix} x \\ 1 \end{bmatrix} \\
&\quad + \begin{bmatrix} x \\ 1 \end{bmatrix}^\top \left(\mathcal{P}(0, \sigma) - e^{\Gamma_\sigma^\top (T_m - \tau)} (\mathcal{P}(0, \sigma) + M) e^{\Gamma_\sigma (T_m - \tau)} \right) \begin{bmatrix} x \\ 1 \end{bmatrix}.
\end{aligned}$$

Recalling the procedure presented in the proof of the periodic time-triggered control case in equation (26) and identifying the event-triggering rule ϕ given in (42), the previous expression can be rewritten as follows

$$\Delta V(x, \tau, \sigma) = \begin{bmatrix} x \\ 1 \end{bmatrix}^\top e^{-\Gamma_\sigma^\top \tau} \left(\Psi_\sigma(T_m) + e^{\Gamma_\sigma^\top T_m} M e^{\Gamma_\sigma T_m} \right) e^{-\Gamma_\sigma \tau} \begin{bmatrix} x \\ 1 \end{bmatrix} + \phi(x, \tau, \sigma)$$

where matrix $\Psi_\sigma(T_m)$ is given in (22) with $T = T_m$.

Following the same techniques as for the periodic time-triggered control case, we note that the previous expression can be rewritten as follows

$$\begin{aligned}
\Delta V(x, \tau, \sigma) &= \begin{bmatrix} x \\ 1 \end{bmatrix}^\top e^{-\Gamma_\sigma^\top \tau} \bar{\Phi}_\sigma(T_m) e^{-\Gamma_\sigma \tau} \begin{bmatrix} x \\ 1 \end{bmatrix} + \phi(x, \tau, \sigma) \\
&\quad - \begin{bmatrix} x \\ 1 \end{bmatrix}^\top e^{-\Gamma_\sigma^\top \tau} (N_\lambda - N_\sigma) e^{-\Gamma_\sigma \tau} \begin{bmatrix} x \\ 1 \end{bmatrix} \\
&\quad - \mu \begin{bmatrix} x \\ 1 \end{bmatrix}^\top e^{-\Gamma_\sigma^\top \tau} \begin{bmatrix} P & h \\ h^\top & h^\top P^{-1} h - 1 \end{bmatrix} e^{-\Gamma_\sigma \tau} \begin{bmatrix} x \\ 1 \end{bmatrix}.
\end{aligned}$$

where we have introduced the notation

$$\bar{\Phi}_i(T_m) = \Psi_\sigma(T) + e^{\Gamma_i^\top T_m} M e^{\Gamma_i T_m} + N_\lambda - N_i + \mu \begin{bmatrix} P & h \\ h^\top & h^\top P^{-1} h - 1 \end{bmatrix}, \quad \forall i \in \mathbb{K}.$$

One may recognize in the second line of the previous equation the expression of Σ_σ given in (28), and the definition of the Lyapunov function in the third

line. This brings us to rewrite the previous expression as follows,

$$\begin{aligned} \Delta V(x, \tau, \sigma) = & \begin{bmatrix} x \\ 1 \end{bmatrix}^\top e^{-\Gamma_\sigma^\top \tau} \bar{\Phi}_\sigma(T_m) e^{-\Gamma_\sigma \tau} \begin{bmatrix} x \\ 1 \end{bmatrix} \\ & - \Sigma_\sigma(x, \tau, \sigma) - \mu(W(x, \tau, \sigma) - 1) + \phi(x, \tau, \sigma). \end{aligned}$$

Hence, we are now ready to ensure the negative definiteness of ΔV . Using a Schur complement to (40), it is guaranteed that $\bar{\Phi}_\sigma(T_m) \prec 0$ hold for any $\sigma \in \mathbb{K}$. Consequently, the first term of the previous expression is negative definite. The second term is negative because of the control law and the third term is also negative since, as for the periodic time-triggered case, this term refers to the assumption that the state, just before a jump occurs, is outside of the attractor. The previous discussion means that there exists a sufficiently small $\varepsilon > 0$ such that

$$\Delta V(x, \tau, \sigma) \leq -\varepsilon \left\| \begin{bmatrix} x \\ \tau \\ \sigma \end{bmatrix} \right\|^2 + \phi(x, \tau, \sigma). \quad (46)$$

Note that this last inequality is made possible since τ is bounded by T_M . According to the definition of the jump set in (33), two cases may occur.

Case I (x, τ, σ) is in $\mathcal{D}_{T_m} \cap \mathcal{D}_e$. This means that $\tau \geq T_m$ and $\phi(x, \tau, \sigma) = 0$.

305 Then, it is clear that $\Delta V(x, \tau, \sigma) \leq -\varepsilon \left\| \begin{bmatrix} x \\ \tau \\ \sigma \end{bmatrix} \right\|^2$.

Case II (x, τ, σ) is in \mathcal{D}_{T_M} . This means that $\tau = T_M$ and $\phi(x, \tau, \sigma) \leq 0$, then (46) holds.

Now, we need to prove the invariance of $\tilde{\mathcal{A}}$ for $(x, \tau, \sigma) \in \tilde{\mathcal{H}}$. From (44), we have $\langle \nabla \tilde{V}(x, \tau, \sigma), \tilde{f}(x, \tau, \sigma) \rangle = 0$, for all (x, τ, σ) in $(\tilde{\mathcal{C}} \cap \tilde{\mathcal{A}}) \subset \tilde{\mathcal{A}}$, which ensures
310 that the solution in the attractor remains in it during flows.

We now need to prove that the solution to $\tilde{\mathcal{H}}$ that enters into $\tilde{\mathcal{A}}$ remains in the attractor during jumps, i.e. $G(\tilde{\mathcal{D}} \cap \tilde{\mathcal{A}}) \subset \tilde{\mathcal{A}}$. To do so, let us note that

condition (20) can be rewritten as follows

$$\begin{aligned}
W(x, 0, \sigma^+) &= W(x, \tau, \sigma) + \Delta W(x, \tau, \sigma) \\
&= W(x, \tau, \sigma) + \begin{bmatrix} x \\ 1 \end{bmatrix}^\top e^{-\Gamma_\sigma^\top \tau} \Phi_\sigma(T_m) e^{-\Gamma_\sigma \tau} \begin{bmatrix} x \\ 1 \end{bmatrix} \\
&\quad - \Sigma_\sigma(x, \tau, \sigma) - \mu(W(x, \tau, \sigma) - 1) + \phi(x, \tau, \sigma) \\
&\leq W(x, \tau, \sigma) - \mu(W(x, \tau, \sigma) - 1) \\
&= (1 - \mu)(W(x, \tau, \sigma) - 1) + 1.
\end{aligned}$$

Then, for any $(x, \tau, \sigma) \in \tilde{\mathcal{A}}$, for which we have $W(x, \tau, \sigma) - 1 < 0$, the assumption $\mu \in (0, 1)$ guaranties $W(x, 0, \sigma^+) < 1$ holds. From its definition, this also means that $V(x, 0, \sigma^+) = 0$. In other words, the previous statement allows us stating what was to be demonstrated, i.e.

$$\Delta V(x, \tau, \sigma) = 0, \quad \forall (x, \tau, \sigma) \in \tilde{\mathcal{D}} \cap \tilde{\mathcal{A}}.$$

As for the periodic event-triggered case, the last step of the proof is to ensure that no complete solution, that are not in \mathcal{A} , keeps constant. This is ensured by the fact that the solution will eventually jump after at most T_M unit of ordinary time. Since, thanks to the previous developments, we have shown that at each
315 jump, the increment of the Lyapunov function is strictly decreasing.

Proof of (ii): The proof of $\tilde{\mathcal{E}} \subset \tilde{\mathcal{A}}$ follows the poof of (ii) in Proof 2. Recall that the set $\tilde{\mathcal{E}}$ is defined by all solutions that start at $x = 0$ just after a jump and evolving in $\tau \in [0, T_m]$. It is easy to see that if LMIs (40) are satisfied, then the particular solutions in $\tilde{\mathcal{E}}$ are in $\tilde{\mathcal{A}}$, as done in the proof of Theorem 1.

320 As noted in Remark 2, the non-convex optimization problem (38)–(40) is transformed in convex, pre-selecting parameter μ by a line-search routine algorithm.

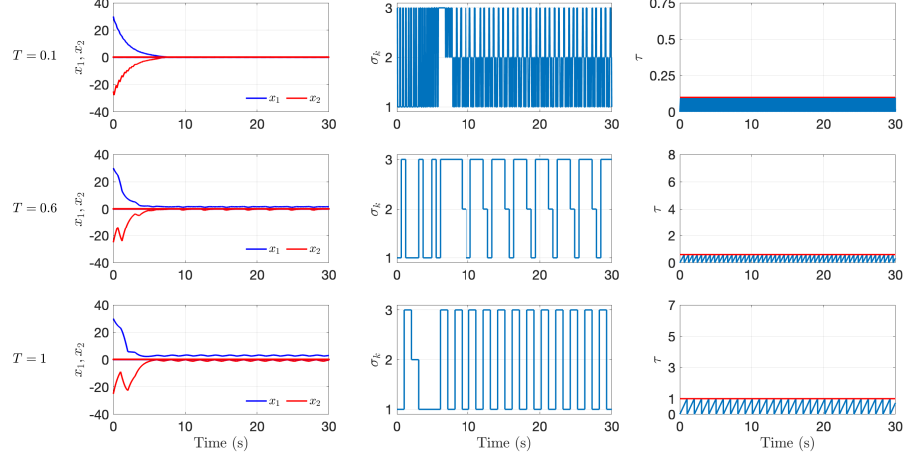


Figure 2: Simulation results of a switched affine system (1), (47) with the periodic time-triggered control for three different values of T , from top to bottom. From left to right, the figure shows the evolution of the state variables (x_1, x_2) , the control input σ and the timer τ .

	μ	$\det(P)^{\frac{1}{2}}$	P	h
T=0.1	0.03	1.03	$\begin{bmatrix} 1.5528 & 0.6818 \\ 0.6818 & 0.9055 \end{bmatrix}$	$\begin{bmatrix} -0.1848 \\ -0.0723 \end{bmatrix}$
T=0.6	0.09	11.21	$\begin{bmatrix} 0.1600 & 0.0473 \\ 0.0473 & 0.0637 \end{bmatrix}$	$\begin{bmatrix} -0.004 \\ -0.002 \end{bmatrix}$
T=1	0.09	20.56	$\begin{bmatrix} -0.0010 & -0.0001 \\ -0.0001 & 0.0014 \end{bmatrix}$	$\begin{bmatrix} -0.0043 \\ -0.0016 \end{bmatrix}$

Table 1: Numerical results for the time-triggered control and for the event-triggered control with $T = T_m$ in the hybrid dynamical formulation (6)–(7) and (30)–(31), respectively.

5. Numerical validation

In this section, we take the system driven by (1) composed by three functioning modes:

$$\begin{aligned}
 A_1 &= \begin{bmatrix} 0 & 0.5 \\ 0 & -1 \end{bmatrix}, & \mathcal{B}_1 &= \begin{bmatrix} 1 \\ 0.5 \end{bmatrix}, \\
 A_2 &= \begin{bmatrix} 0.1 & 0 \\ -1 & -1 \end{bmatrix}, & \mathcal{B}_2 &= \begin{bmatrix} -1 \\ -0.5 \end{bmatrix}, \\
 A_3 &= \begin{bmatrix} 0 & 1 \\ -1 & 0 \end{bmatrix}, & \mathcal{B}_3 &= \begin{bmatrix} 0 \\ 2 \end{bmatrix}.
 \end{aligned} \tag{47}$$

The desired equilibrium is $z_e = [0.1 \ 0.2]^T$ associated with $\lambda = [0.40 \ 0.47 \ 0.13]$ belongs to Ω_e . Note that the each functioning mode is instable.

We consider the following switching times for the time-triggered control (2) as well as the minimum dwell times for the event-triggered control (3): $T =$

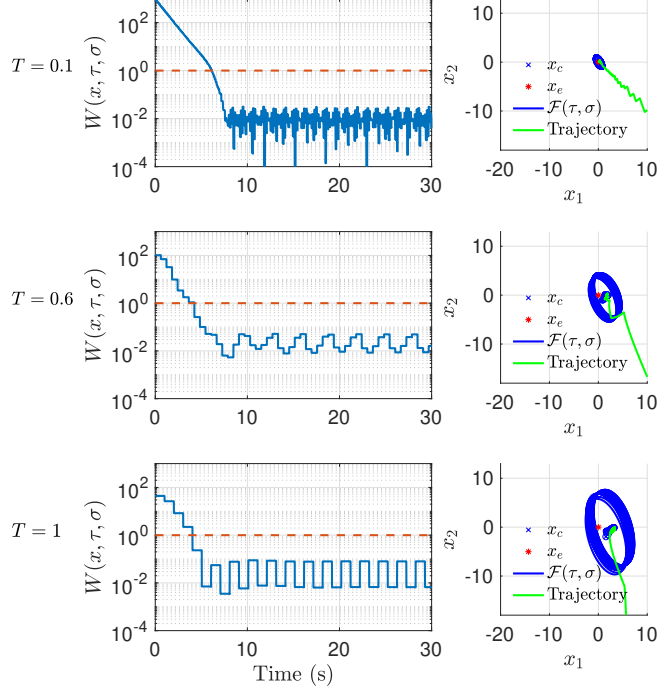


Figure 3: Simulation results of a switched affine system (1), (47) with the periodic time-triggered control for three different values of T , from top to bottom. From left to right, the figure shows the function $W(x, \tau, \sigma)$ (in a logarithmic scale), with respect to time and the second column shows the trajectories of the state space x and the projection of \mathcal{A} in x , i.e. $\mathcal{F}(\tau, \sigma)$.

$T_m = 0.25, 0.5$ and 1 s. The maximum dwell-time is arbitrarily selected as $T_M = 100$ s. As mentioned in Remark 2, numerical results have been obtained on
330 MATLAB by performing a line-search algorithm on parameter $\mu \in (0, 1)$, and then solving the resulting convex optimization using the CVX sdp solver [36].

We first stress that the optimal solutions obtained from both Theorems 1 and 2 are the same given in Table 1, even though the conditions are different, because of matrix M in the event-triggered case. Looking at the numerical
335 values, matrix M is of order 10^{-10} in all cases. Therefore, comparatively to the values of P given in Table 1, its influence can be neglected. This can be expected from the LMI conditions since the only constraint on M is to be positive definite.

5.1. Comments on the periodic time-triggered control

On the one hand, some simulations are performed when the periodic time-triggered control law given in (2) is applied to system (1) via the hybrid dynamical system (6)–(7), with the parameters computed from the optimization
340

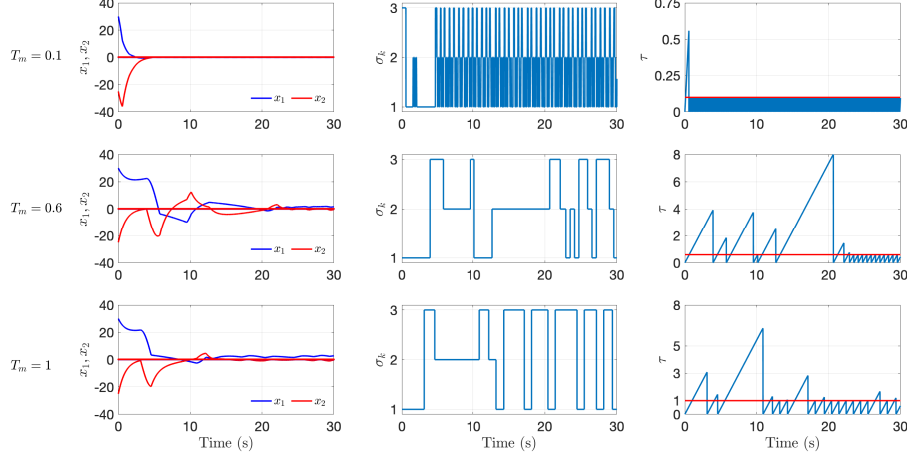


Figure 4: Simulation results of a switched affine system (1), (47) with the aperiodic time-triggered control for three different values of T_m , from top to bottom. From left to right, the figure shows the evolution of the state variables (x_1, x_2) , the control input σ and the timer τ .

problem given in Theorem 1. Figure 2 shows the time evolution of the state x , the control input σ and the timer τ . Note in the second column of Figure 2, that the achieved operating point and its associated weighting vector are different to the pair (z_e, λ) . Indeed, the system converges asymptotically to a neighborhood of the origin, evolving in the hybrid time domain (10), as hybrid arcs. The last column shows timer τ bounded by T , driving to periodic-time switching.

Figure 3, shows, in the first column, the convergence of the solutions to \mathcal{A} , which is illustrated through the graph of $W(x, \tau, \sigma)$. Indeed, the solutions enter into \mathcal{A} when $W(x, \tau, \sigma)$ is lower than 1. In the second column, we highlight more insights on the attractor. To do so, let us introduce the following function \mathcal{F} from $[0, T] \times \mathbb{K}$ to \mathbb{R}^n , which represents the boundary of the attractor \mathcal{A} projected on the state space x . More formally, let us define \mathcal{F} as follows

$$\mathcal{F}(\tau, \sigma) := \{x \in \mathbb{R}^n, \quad W(x, \tau, \sigma) = 1\}, \quad \forall (\tau, \sigma) \in [0, T] \times \mathbb{K}.$$

It is worth noting that the graph of $\mathcal{F}(\tau, \sigma)$ draws, for each value of τ and σ , an ellipsoid. It can be seen that the increasing of T implies an expected increase of the volume of $\mathcal{F}(\tau, \sigma)$ independently of τ and σ . This increase of \mathcal{A} is also appreciated in Table 1, which provides an estimation of the volume of the ellipse drawn by the attractor when $\tau = 0$ (and independent of σ), which is proportional to $\det(P)^{-\frac{1}{2}}$. It is noted as the origin remains in the interior of \mathcal{A} .

5.2. Comments on the aperiodic event-triggered control

The same simulation setup has been considered in the aperiodic event-triggered case. Similarly to the periodic case, Figure 4 shows the state evolutions, when the event-triggered control (3) is applied to system (1), via the

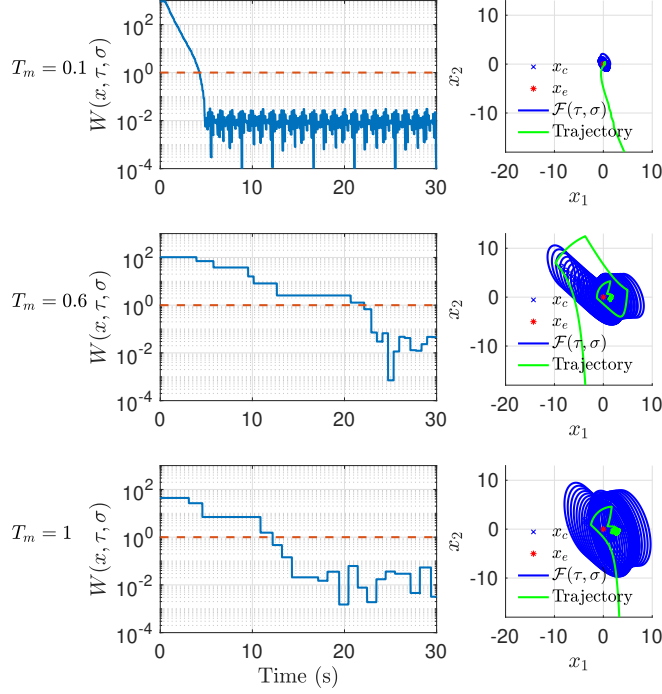


Figure 5: Simulation results of a switched affine system (1), (47) with the aperiodic time-triggered control for three different values of T_m , from top to bottom. From left to right, the figure shows the function $W(x, \tau, \sigma)$ (in a logarithmic scale), with respect to time and the second column shows the trajectories of the state space x and the projection of $\tilde{\mathcal{A}}$ in x .

hybrid dynamical system (30)–(31) with three a priori selected minimum dwell times $T_m = 0.1, 0.6$ and 1 . It is appreciated as the timer, τ , generates an aperiodic switching rule between the minimum dwell time T_m and the maximum dwell time T_M selected arbitrarily as 100 .

Comparing the simulation results of Figure 2 with respect to Figure 4, which were performed for the same initial conditions, we first remark that the solutions to the systems also converge in a neighborhood of the origin. However, one can also note that the transient period is larger in the event-triggered case compared to the time-triggered one. We can see in the last column of the figure that the timer reach a periodic behavior once the solutions are close to the equilibrium. Before that, we can see in these simulations that the solutions to the event-triggered controller are able to flow during a notable while (up to 8 units of ordinary time). Therefore, the event-triggered control law is able to reduce the number of control updates compared to the periodic time-triggered case.

Figure 5 depicts the evolution of $W(x, \tau, \sigma)$ (first column) and the projection of $\tilde{\mathcal{A}}$ into the space x (in the second column). While the optimization problem

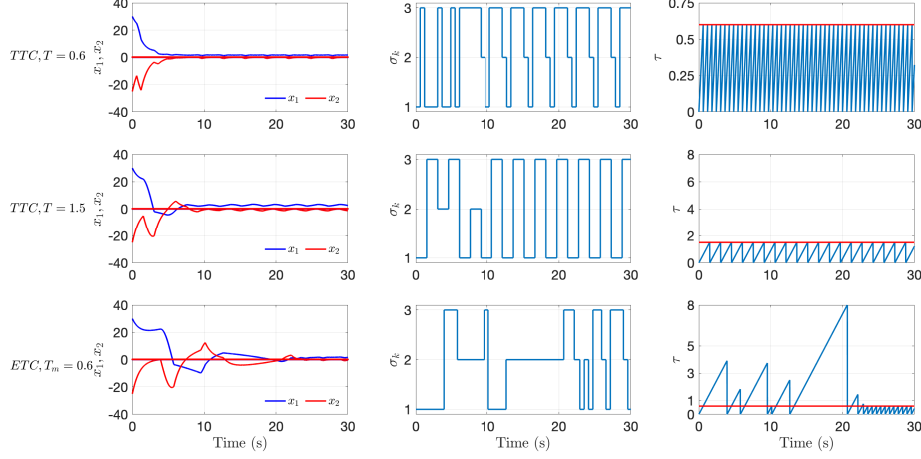


Figure 6: Simulations presenting the evolution of the state x (left), the selected mode σ (middle) and the timer τ (right) for two time-triggered controller (TTC) with $T = 0.6$ and 1.5 and for the event-triggered case (ETC) with $T_m = 0.6$.

presented in both theorems delivers the same values, the fact that the timer is allowed to reach larger values than the minimum dwell time. This leads to notable differences when plotting the projection of attractor $\tilde{\mathcal{A}}$. Indeed the graphs of $\mathcal{F}(\tau, \sigma)$ for each values of the minimum dwell time T_m presents larger variations compared to the periodic case. However, since the simulations show that the timer seems to converge to a periodic behavior of period T_m , the projections of the attractor in the steady state in both time- and event-triggered converge to the same region.

5.3. Fair comparison between both approaches

When comparing the solutions to the time- and event-triggered controller, it seems that the best performances are achieved by the periodic time-triggered. Indeed, for this set of simulations, the transient of the time-triggered case are shorter than the ones of the event-triggered case, when comparing the solutions with $T = T_m$. However, this comparison is not really fair, since in the periodic solutions requires more control actions than the aperiodic one.

In order to provide a more accurate comparison, let us focus on the solution of the event-triggered case with $T_m = 0.6$. The triggering rule generates 19 events corresponding to a change of mode over a simulation of 30s. Therefore, an equivalent periodic control for this simulation would requires to select $T = 30/19$, for which no solution to the optimization problem of Theorem 1 can be found. However, a solution has been obtained for a slightly lower value $T = 1.5$. Figure 6 now illustrates a fair comparison where the solution to the periodic time-triggered controller with $T = 0.6$ and 1.5 and to the event-triggered controller with $T_m = 0.6$ are presented. Indeed, the two simulations at the bottom of the figure have the same number of control updates. Even though the

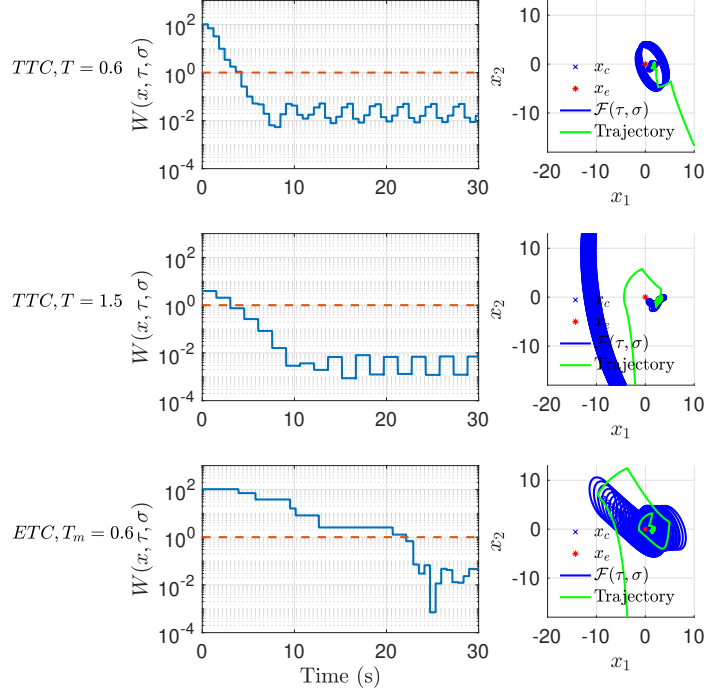


Figure 7: Simulations presenting the evolution of $W(x, \tau, \sigma)$ (left) and the solutions to the system in the phase plan (right) for two time-triggered controller (TTC) with $T = 0.6$ and 1.5 and for the event-triggered case (ETC) with $T_m = 0.6$.

transient of the periodic solution is shorter than the aperiodic one, the solution
to the periodic case has a larger chattering around the equilibrium compared
to the aperiodic case. Moreover, the guarantees of the periodic controller with
 $T = 1.5$ are much worse than the aperiodic one as shown in Figure 7, where the
projection of the attractor is way much larger than the aperiodic case. There-
fore, in light of the previous comments, the event-triggering controller has the
merit to reduce the number of control updates while keeping the same guaran-
tees on the size of the attractor, but at the price of reducing the performance
during the transient phase.

6. Conclusions and perspectives

This work presents a switching controller for affine systems, defined by
continuous-time and discrete-time dynamics, when the input signal is periodi-
cally or aperiodically updated. The main result presented here provides a control
with a simple structure, which is not structured in the system matrices. It is
proven UGAS of a compact attractor defined in the hybrid state space (x, τ, σ)

and the practical asymptotic stability of the operating point $z_e = z - x$. A deep
415 discussions has been proposed in the numerical application sections and shows
the advantages and drawbacks of each control strategies. In future work, we
aim at exploiting this framework to ensure the robustness of the system with
respect to parameter variations and to jitter.

Acknowledgments

420 This work has been partially funded under grant “HISPALIS” ANR-18-
CE40-0022-01.

References

- [1] D. Liberzon, Switching in systems and control, Springer Science & Business Media, 2012.
- 425 [2] H. Sira-Ramírez, R. Silva-Ortigoza, Control design techniques in power electronics devices, Springer Science & Business Media, 2006.
- [3] T. Theunisse, J. Chai, R. Sanfelice, W. Heemels, Robust global stabilization of the dc-dc boost converter via hybrid control, IEEE Trans. on Circuits and Systems I: Regular Papers 62 (4) (2015) 1052–1061.
- 430 [4] F. Parise, M. E. Valcher, J. Lygeros, Computing the projected reachable set of stochastic biochemical reaction networks modelled by switched affine systems, IEEE Trans. on Automatic Control (2018).
- [5] B. Oh, J. Jeong, J. Suk, S. Kim, Design of a control system for an organic flight array based on a neural network controller, International Journal of Aerospace Engineering (2018).
- 435 [6] M. Hajiahmadi, B. De Schutter, H. Hellendoorn, Robust h-infty switching control techniques for switched nonlinear systems with application to urban traffic control, International Journal of Robust and Nonlinear Control 26 (6) (2016) 1286–1306.
- 440 [7] S. Pettersson, B. Lennartson, Stabilization of hybrid systems using a min-projection strategy, in: Proc. of the 2001 IEEE American Control Conference, Vol. 1, 2001, pp. 223–228.
- [8] C. Seatzu, A. Corona, D. Giua, A. Bemporad, Optimal control of continuous-time switched affine systems, IEEE Trans. on Automatic Control 51 (5) (2006) 726–741.
- 445 [9] C. Albea, G. Garcia, L. Zaccarian, Hybrid dynamic modeling and control of switched affine systems: application to dc-dc converters, in: 2015 54th IEEE Conference on Decision and Control (CDC), IEEE, 2015, pp. 2264–2269.

- 450 [10] G. Deaecto, J. Geromel, F. Garcia, J. Pomilio, Switched affine systems control design with application to DC-DC converters, *IET control theory & applications* 4 (7) (2010) 1201–1210.
- [11] L. Egidio, H. Daiha, G. Deaecto, J. Geromel, DC motor speed control via buck-boost converter through a state dependent limited frequency switching rule, in: *Proc. of the IEEE Annual Conference on Decision and Control* (CDC), IEEE, 2017, pp. 2072–2077.
- 455 [12] A. Sferlazza, C. Albea-Sanchez, L. Martínez-Salamero, G. Garcia, C. Alonso, Min-type control strategy of a DC-DC synchronous boost converter, *IEEE Transactions on Industrial Electronics* (2019). doi:10.1109/TIE.2019.2908597.
- 460 [13] Y. Lu, W. Zhang, A piecewise smooth control-lyapunov function framework for switching stabilization, *Automatica* 76 (2017) 258–265.
- [14] J. Buisson, P. Richard, H. Cormerais, On the stabilisation of switching electrical power converters, in: *Hybrid Systems: Computation and Control*, Vol. 3414 of *Lecture Notes in Computer Science*, Springer Berlin Heidelberg, 2005, pp. 184–197.
- 465 [15] M. Senesky, G. Eirea, T. Koo, Hybrid modelling and control of power electronics, in: *Hybrid Systems: Computation and Control*, Vol. 2623 of *Lecture Notes in Computer Science*, Springer Berlin Heidelberg, 2003, pp. 450–465.
- 470 [16] C. Albea Sanchez, G. Garcia, S. Hadjeras, M. W. P. M. H. Heemels, L. Zaccarian, Practical stabilisation of switched an systems with dwell-time guarantees, *IEEE Trans. on Automatic Control* (2109). doi:10.1109/TAC.2019.2907381.
- 475 [17] P. Colaneri, J. C. Geromel, A. Astolfi, Stabilization of continuous-time switched nonlinear systems, *Systems & Control Letters* 57 (1) (2008) 95–103.
- [18] J. Liu, X. Liu, W. Xie, On the (h_0, h) -stabilization of switched nonlinear systems via state-dependent switching rule, *Applied Mathematics and Computation* 217 (5) (2010) 2067–2083.
- 480 [19] M. Kumar, R. Gupta, Sampled time domain analysis of digital pulse width modulation for feedback controlled converters, *IET Circuits, Devices & Systems* 10 (6) (2016) 481–491.
- [20] X. Sun, X. Li, Y. Shen, B. Wang, X. Guo, Dual-bridge LLC resonant converter with fixed-frequency PWM control for wide input applications, *IEEE Trans. Power Electron* 32 (1) (2017) 69–80.
- 485 [21] F. Bernelli-Zazzera, P. Mantegazza, Pulse-width equivalent to pulse-amplitude discrete control of linear systems, *Journal of guidance, control, and dynamics* 15 (2) (1992) 461–467.

- 490 [22] S. Ibrir, W. Xie, C. Su, Observer-based control of discrete-time lipschitzian non-linear systems: application to one-link flexible joint robot, *International Journal of Control* 78 (6) (2005) 385–395.
- [23] P. Nino-Suarez, E. Aranda-Bricaire, M. Velasco-Villa, Discrete-time sliding mode path-tracking control for a wheeled mobile robot, in: *Proc. of the IEEE Conference on Decision and Control (CDC)*, 2006, pp. 3052–3057.
- 495 [24] P. Hauvoigne, P. Riedinger, C. Iung, Switched affine systems using sampled-data controllers: Robust and guaranteed stabilisation, *IEEE Trans. on Automatic Control* 56 (12) (2011) 2929–2935.
- [25] G. Deaecto, J. Geromel, Stability analysis and control design of discrete-time switched affine systems, *IEEE Trans. on Automatic Control* 62 (8) (2017) 4058–4065.
- 500 [26] C. Albea Sanchez, A. Ventosa-Cutillas, A. Seuret, F. Gordillo, Robust switching control design for uncertain discrete-time switched affine systems., Submitted to *International Journal of Robust Nonlinear Control* (2019).
- 505 [27] R. Goebel, R. Sanfelice, A. Teel, *Hybrid Dynamical Systems: modeling, stability, and robustness*, Princeton University Press, 2012.
- [28] L. Torquati, R. Sanfelice, L. Zaccarian, A hybrid predictive control algorithm for tracking in a single-phase DC-AC inverter, in: *proc. IEEE Control Technology and Applications (CCTA)*, 2017, pp. 904–909.
- 510 [29] L. Hetel, C. Fiter, H. Omran, A. Seuret, E. Fridman, J.-P. Richard, S.-I. Niculescu, Recent developments on the stability of systems with aperiodic sampling: An overview, *Automatica* 76 (2017) 309–335.
- [30] L. Hetel, E. Fridman, Robust sampled-data control of switched affine systems, *IEEE Trans. on Automatic Control* 58 (11) (2013) 2922–2928.
- 515 [31] C. Edwards, S. Spurgeon, *Sliding mode control: theory and applications*, Crc Press, 1998.
- [32] A. Cutillas, C. Albea Sanchez, A. Seuret, F. Gordillo, Relaxed periodic switching controllers of high-frequency DC-DC converters using the δ -operator formulation, in: *Proc. of the IEEE Conference on Decision and Control*, 2018, pp. 3433–3438.
- 520 [33] A. Seuret, C. Prieur, S. Tarbouriech, A. Teel, L. Zaccarian, A nonsmooth hybrid invariance principle applied to robust event-triggered design, *IEEE Trans. on Automatic Control* 64 (5) (2018) 2061–2068.
- 525 [34] C. Briat, Convex conditions for robust stabilization of uncertain switched systems with guaranteed minimum and mode-dependent dwell-time, *Systems & Control Letters* 78 (2015) 63–72.

- 530
- [35] J. Jin, J. Ramirez, S. Wee, D. Lee, Y. Kim, N. Gans, A switched-system approach to formation control and heading consensus for multi-robot systems, *Intelligent Service Robotics* 11 (2) (2018) 207–224.
 - [36] M. Grant, S. Boyd, CVX: Matlab software for disciplined convex programming, version 2.1 (2014).